Eur. Phys. J. A **11**, 125–136 (2001)

THE EUROPEAN PHYSICAL JOURNAL A

Charge-independent effective interactions for shell-model studies in the $0g_{9/2}$-$1p_{1/2}$ space

I.P. Johnstone[1] and L.D. Skouras[2,a]

[1] Department of Physics, Queen's University, Kingston, Ontario, Canada K7L 3N6
[2] Institute of Nuclear Physics, N.C.S.R. Demokritos, GR-15310 Aghia Paraskevi, Greece

Received: 31 May 2001
Communicated by P. Schuck

Abstract. The matrix elements of the effective Hamiltonian in the $0g_{9/2}$-$1p_{1/2}$ space are determined by a least-square fit to the energies of 477 levels of nuclei with $38 \leq Z \leq 50$ and $47 \leq N \leq 50$. The results of the calculation are found to be in better agreement with experiment than those obtained with previously determined interactions.

PACS. 21.60.Cs Shell model – 21.30.Fe Forces in hadronic systems and effective interactions – 21.10.Dr Binding energies and masses

1 Introduction

Early shell-model studies [1–7] of nuclei with $N = 50$ neutrons and proton number Z in the range $38 \leq Z \leq 50$ assumed an inert $^{88}_{38}$Sr core and placed the valence protons in the $0g_{9/2}$ and $1p_{1/2}$ orbitals of a harmonic oscillator. Later, this model was extended to describe nuclei with $N < 50$ neutrons [8,9]. In this case the $50 - N$ neutrons were treated as holes to ^{88}Sr occupying, again, the $g_{9/2}$ and $p_{1/2}$ orbitals. Since then calculations in the $g_{9/2}$-$p_{1/2}$ space[1] were performed for a variety of nuclei with $38 \leq Z, N \leq 50$, both in order to interpret observed level schemes and electromagnetic transitions [10–27] but also to make predictions about the β^+ decay of the proton-rich nuclei in the vicinity of ^{100}Sn [28–31].

Of course, there is experimental evidence[2] that the *gp*-space is not adequate to describe all observed properties of the $38 \leq Z, N \leq 50$ nuclei. Such evidence is provided, for example, by the presence of low-lying $3/2^-$ and $5/2^-$ states in the spectra of ^{87}Sr, ^{89}Y and ^{91}Nb and of the observed high-spin states in ^{92}Ru [33], ^{94}Rh [34], ^{93}Tc, ^{94}Ru and ^{95}Rh [35]. To describe such data, there have been attempts to enlarge the model space either by including the $1p_{3/2}$ and $0f_{5/2}$ orbitals [36–38] or by allowing particle-hole excitations from the *gp*-space to the $0g_{7/2}, 1d_{5/2}, 2s_{1/2}, 1d_{3/2}$ orbitals above [39,40]. However, the problem with these large model spaces is that the energy matrices have exceedingly large dimensions, specially if both Z and N differ from the magic number 50. It is for this reason, but also for the fact that most nuclear properties are satisfactorily reproduced in the *gp*-space, that calculations employing this simple model are still widely used for the study of nuclei in the ^{100}Sn region [10–31].

The success of shell-model calculations in the *gp*-space can be attributed to two successful determinations of the effective interaction which is appropriate for this space. Both these interactions were derived [7–9] by a least-square fit of the matrix elements of the Hamiltonian to the energy levels of several $N = 50$ and $N = 49$ nuclei.

The first of these interactions, to be hereafter named SLG, was derived in two steps. In the first step Gloeckner and Serduke [7] determined the nine 2-body proton matrix elements and the two-proton single-particle energies, relative to ^{88}Sr, by fitting them to 45 energy levels of $N = 50$ nuclei. The second step involved the determination of the proton-neutron interaction which was accomplished by a least-square fit to 63 energy levels of $N = 49$ nuclei [8]. Here the neutron-hole energies were taken from the experimental spectrum of ^{87}Sr, while the proton part of the Hamiltonian was that of ref. [7]. Several versions of the 2-body interaction were derived in ref. [8]. The one which produces best agreement with experiment does not conserve isospin, since the $\langle p_\pi g_\nu | V | p_\pi g_\nu \rangle$ and $\langle g_\pi p_\nu | V | g_\pi p_\nu \rangle$ matrix elements were treated as independent parameters, which took different values. There is, however, another version of the SLG 2-body interaction which does conserve isospin. This interaction, to be distinguished in the

[a] e-mail: skouras@mail.demokritos.gr

[1] In the following we use, for brevity, the term *gp*-space instead of $g_{9/2}$-$p_{1/2}$ space. In formulae and tables, we also use p for $p_{1/2}$ and g for $g_{9/2}$, while π and ν denote protons and neutrons, respectively.

[2] Unless otherwise stated, all experimental information used in this work is from the compilation of NNDC [32].

following as SLGT, was derived by treating as parameters the 9 $T = 0$ matrix elements which exist in the *gp*-space [8]. The 9 $T = 1$ matrix elements were then taken from the proton-proton interaction of ref. [7] by removing the Coulomb contribution [8]. Thus, the SLGT interaction can be used for studies of nuclei with $N < 49$. This feature does not apply to the isospin non-conserving SLG interaction, since the latter does not contain a 2-neutron part.

The SLGT interaction was recently used by Herndl and Brown [26] in a shell-model study of several nuclei in the $38 \leq Z, N \leq 50$ range. In contrast, however, to the original SLGT method, Herndl and Brown ignored the 2-body Coulomb interaction, while they used common single-particle energies for protons and neutrons. Their results, therefore, are obtained in isospin formalism. Binding energies are obtained by adding the shell-model energy to the contribution of a 5-parameter formula, which they fit to the experimental ground-state energies [26].

The other interaction widely used in the *gp*-space was derived by Gross and Frenkel [9]. This interaction, to be herafter called GF, was obtained by a least-square fit to 95 energies of several $N = 50$ and $N = 49$ nuclei and of some levels of the $N = 48$ nucleus ^{86}Sr. Gross and Frenkel [9] considered 33 parameters in their fit, *i.e.* 4 single-particle energies, 9 2-proton matrix elements and the 20 matrix elements which describe the interaction of a proton with a neutron hole. However, their interaction approximately conserves isospin, since they introduced appropriate constraints in the variation of their parameters [9]. Thus, the GF interaction, like the SLGT, can be used in shell-model studies of $N \leq 48$ nuclei. Recently, this interaction has become very popular among experimentalists [13–23,27], who want to compare their results with shell-model predictions.

Both the SLG and GF interactions were determined about 25 years ago, *i.e.* at a time when the experimental information on the $38 \leq Z, N \leq 50$ nuclei was much more restricted than the existing nowadays. Since then only few attempts have been made to include more data in the determination of the effective interaction and these were restricted to the proton interaction only [11,41].

In the present work an attempt is made to derive a charge-independent effective interaction which is appropriate for shell-model calculations in the *gp*-space. The method followed is similar to that of the SLG [7,8] and GF [9] calculations, but the number of experimental data considered here, about 500, is much larger than those considered in the two earlier fits. Moreover, these data include information on $N = 47, 48$ nuclei but also on proton-rich nuclei like ^{98}Cd, ^{97}Ag, $^{94\text{-}96}$Pd, $^{92\text{-}95}$Rh etc., *i.e.* nuclei which are outside the range of those treated in the SLG and GF investigations.

Details of the calculation are given in sect. 2 while the results of the calculation are presented in sect. 3. Finally, sect. 4 contains some discussion on our work.

Table 1. Coulomb matrix elements (in keV).

Matrix element	J	Value
$\langle g^2\|V\|g^2\rangle$	0	338
	2	292
	4	263
	6	250
	8	252
$\langle g^2\|V\|p^2\rangle$	0	−14
$\langle gp\|V\|gp\rangle$	4	268
	5	274
$\langle p^2\|V\|p^2\rangle$	0	309

2 Description of the calculation

Our determination of the effective interaction follows closely the SLGT approach [8]. Thus, charge independence of the nuclear interaction is directly introduced in the calculation by expressing the 2-body matrix elements in isospin formalism. There are 18 2-particle (hole) matrix elements in the *gp*-space and these are treated as parameters to be determined by the least-square fit procedure. All other required 2-body matrix elements, like the proton-neutron or proton-proton interactions, are at each stage of the calculation related to the 18 isospin elements. The 2-proton interaction, in particular, is obtained by adding to the $T = 1$ matrix elements the Coulomb contributions listed in table 1.

There are 4 more parameters considered in the calculation which correspond to single-particle energies. In our approach we assume the doubly magic nucleus $^{100}_{50}$Sn as inert core and describe all nuclei in the range $38 \leq Z, N \leq 50$ in terms of $50 - Z$ proton and $50 - N$ neutron holes. Thus the 4 extra parameters describe the 2-proton and the 2-neutron single-hole energies relative to ^{100}Sn.

The selection of ^{100}Sn as core was made because it offers a more symmetric treatment of protons and neutrons. It has, also, the practical advantage that one does not need to transform, at each stage of the calculation, the 2-body interaction to the particle-hole representation, which is required with a ^{88}Sr core. Such a transformation is accomplished by means of the Pandya relation [42]

$$\langle j_1, j_2^{-1}; J|V|j_3, j_4^{-1}; J\rangle = -\sum_L (2L+1) \begin{Bmatrix} j_1 & j_2 & J \\ j_3 & j_4 & L \end{Bmatrix} \langle j_1, j_4; L|V|j_3, j_2; L\rangle \,. \quad (1)$$

Generally, the choice of ^{100}Sn or ^{88}Sr as core produces no difference on the final results. However, a practical difference occurs if one wants to follow the SLG approach [8] and use the ^{87}Sr experimental energies, given by

$$\epsilon^{\nu}_{9/2} = 11.113 \text{ MeV}, \qquad \epsilon^{\nu}_{1/2} = 11.501 \text{ MeV} \quad (2)$$

in order to fix the single-neutron hole energies relative to ^{88}Sr. In our approach the reproduction of the ^{87}Sr energies can be accomplished by introducing, as constraints

between the parameters, the following equation:

$$E_j^\nu + \frac{1}{2j+1}\sum_{l=p,g}\sum_J (2J+1)\langle j_\nu l_\pi; J|V|j_\nu l_\pi; J\rangle = \epsilon_j^\nu \ , \quad (3)$$

where E_j, $j = 9/2, 1/2$, represents the single-hole energy relative to ^{100}Sn, ϵ_j^ν are defined in eq. 2, while the proton-neutron matrix elements are related to the parameters of the calculation $\langle jl; JT|V|jl; JT\rangle$. In a similar fashion to eq. (3), one can also introduce constraint equations which help to reproduce the ^{89}Y energies relative to ^{88}Sr. These are:

$$E_j^\pi + \frac{1}{2j+1}\sum_{l=p,g}(1+\delta_{jl})\sum_J (2J+1)\langle jl; J|V|jl; J\rangle = -\epsilon_j^\pi - \frac{1}{2j+1}\sum_{l=p,g}(1+\delta_{jl})\sum_J (2J+1)\langle jl; J|C|jl; J\rangle . \quad (4)$$

In the above equation $\langle jl; J|V|jl; J\rangle$ are the nuclear matrix elements between two protons in orbits j, l, $\langle jl; J|C|jl; J\rangle$ the corresponding Coulomb elements, while ϵ_j^π represent the ^{89}Y energies relative to ^{88}Sr, *i.e.*

$$\epsilon_{9/2}^\pi = -6.162 \ \text{MeV} , \qquad \epsilon_{1/2}^\pi = -7.071 \ \text{MeV} . \quad (5)$$

The 22 parameters of our calculation were determined by a least-square fit to the experimental data of $38 \le Z \le 50$ and $47 \le N \le 50$ nuclei. Details of the fitting procedure are given in the book of Brussaard and Glaudemans [43] and need not be repeated here. The quantity which is minimized is the χ^2 defined [9] as

$$\chi^2 = \sum_{i=1}^{D}(E_i^{\rm exp} - E_i^{\rm cal})^2 + \sum_{j=1}^{4} w_j \Delta_j^2 , \quad (6)$$

where D is the number of experimental data, while $E^{\rm exp}$ and $E^{\rm cal}$ represent experimental and calculated energies, respectively. The second term on the r.h.s of eq. (6) takes care of the 4 constraints defined in eqs. (3)-(4). Here Δ_j is the deviation between the l.h.s and the r.h.s of constraint j [9], while w_j is the weight factor. We use a different weight for each constraint which can take the values 0 (no constraint) or 1000.

The quality of the fit can be measured by the *root-mean-square deviation* [43]

$$\text{rms} = \sqrt{\frac{\chi^2}{D-P}} , \quad (7)$$

where P is the number of parameters. However, to compare our results with other calculations, where different number of parameters and constraints are used, we prefer to consider the *mean level deviation* [9]

$$\text{mld} = \sqrt{\frac{\chi^2}{D}} . \quad (8)$$

In our initial attempt to fit the effective interaction for the *gp*-space, we considered a set of 519 experimental data. These data consisted of binding energies [44] and excitation energies [13,22,23,32–34,45]of the following 36 nuclei: $^{85\text{-}87}$Sr, $^{86\text{-}89}$Y, $^{87\text{-}90}$Zr, $^{88\text{-}91}$Nb, $^{89\text{-}92}$Mo, $^{90\text{-}93}$Tc, $^{91\text{-}94}$Ru, $^{92\text{-}95}$Rh, $^{94\text{-}96}$Pd, ^{97}Ag and ^{98}Cd. The 519 data can also be distributed in the following way: 91 correspond to $N = 50$ nuclei, 120 to $N = 49$, 149 to $N = 48$, while the remaining 159 to $N = 47$ nuclei. Finally, it should be mentioned that the experimental data considered in our work contained levels of both definite and tentative spin-parity assignments. The latter were included under the condition that they could be reproduced within 1 MeV by the SLGT and GF interactions.

The results of this first calculation were not satisfactory, despite the fact that the obtained mld = 169 keV is considerably smaller than the 228 keV and 222 keV values obtained, for the same data, with the SLGT and GF interactions. Thus there were some large deviations between experimental and calculated energies, which in certain cases were of the order of 650 keV. Most of these large deviations occured for states with tentative J^π assignements, like the possible $35/2^+$ and $41/2^+$ states of ^{93}Rh at 5.157 and 6.922 MeV or the possible 10^+ of ^{86}Y at 1.326 MeV. There were, however, also states with definite J^π assignments, like the 2^+ of ^{86}Sr at 1.077 MeV and the $7/2^+$ of ^{85}Sr at 232 keV, for which the calculated energies were about 500 keV too high. In view of the fact that in the ^{87}Sr spectrum there are low-lying $3/2^-$ and $5/2^-$ states, one cannot exclude the possibility that the low-lying states of the ^{85}Sr and ^{86}Sr contain large admixtures from configurations outside the *gp*-space.

It is well known [8,9] that the inclusion in the fitting procedure of data which are not well described in the chosen model space, produces a general deterioration of the other results. For this reason, we removed from the fitting procedure all data for which there was a large deviation between experimental and calculated values. This elimination, which was accomplished in several steps, resulted in a set of 477 experimental data which can be satisfactorily reproduced by the calculation. From these 477 data, 85 correspond to $N = 50$ nuclei, 114 to $N = 49$, 139 to $N = 48$ and 139 to $N = 47$.

At this point, it should be mentioned that the removal of the 42 levels from the original experimental data set of 519, described above, was not always a well-defined procedure. Thus, there were several levels among those 42, which could be satisfactorily reproduced if a smaller number of nuclei was considered in the fitting calculation. This is the case, for example, with the 12 removed $N = 50, 49$ levels. As discussed below, these 12 levels can be satisfactorily reproduced in a fitting calculation where only $N = 50, 49$ nuclei are examined.

A general survey of the results obtained from the fitting of the 477 levels, discussed above, is shown in table 2, where results obtained with other effective interactions [8,9,26] are also included for comparison. Table 2 shows the distribution of the 477 levels into various energy intervals. Each interval represents the range of deviation between experimental and calculated levels. The two columns marked as F-FIT and C-FIT in table 2

Table 2. Quality of the 477 level fit.

Deviation in keV	Number of levels				
	F-FIT	C-FIT	GF	SLGT	ref. [26]
0–50	164	157	124	123	99
51–100	103	104	84	85	98
101–150	88	89	77	78	77
151–200	58	55	57	58	63
201–250	34	43	40	42	28
251–300	27	23	40	27	36
301–350	2	5	17	22	23
351–400	1	0	14	11	16
401–500	0	1	17	18	18
> 500	0	0	7	13	19
mld	128	131	198	206	226

correspond to two different determinations of the effective interaction which are described below.

The F-FIT (free fit) interaction was obtained without using any constraints. The results of this calculation produce the lowest mld value of 128 keV, while they reproduce 474 out of the 477 data within 300 keV. In fact, the vast majority of results obtained in the F-FIT calculation are within 200 keV from the experimental data. As table 2 shows, there are only three levels in the F-FIT results for which the deviation from experiment is larger than 300 keV. The first of these is the 6^+ state of ^{98}Cd, which the calculation produces 307 keV too high, while the other two are the 0^+ state of ^{88}Y at 766 keV, calculated to be 318 keV too low, and the $1/2^-$ state of ^{87}Sr at 389 keV which the calculation predicts to be only 14 keV above the ground state. This last result is rather disappointing, since one of the basic assumptions of the $g_{9/2}$-$p_{1/2}$ model is that ^{87}Sr is a 1-neutron hole nucleus with respect to ^{88}Sr. It was because of this assumption that the $1/2^-$ state of ^{87}Sr was not removed from the data considered in the fitting procedure.

To correct the ^{87}Sr situation, we have attempted another calculation, marked as C-FIT (constrained fit) in table 2, in which the constraints (3) were considered in the fitting procedure. The results of this last calculation reproduce within 1 keV the ^{87}Sr spectrum. However, as table 2 shows, the mld value is increased to 131 keV, while there is a level which now deviates from experiment by more than 400 keV. This is the 0^+ state of ^{88}Y, discussed above, which the C-FIT calculation produces 478 keV too low. Not shown in table 2 are the results of a third calculation in which all constraints (3) and (4) were considered and which produces mld = 136 keV. Since, however, the ^{89}Y experimental levels are reproduced within 150 keV by both F-FIT and C-FIT calculations the inclusion of the type (4) constraints was not considered necessary.

As table 2 shows, the mld values corresponding to results obtained with the SLGT [8] and GF [9] interactions are considerably larger than our results. This is easily understood, since the set of experimental data considered in our fitting procedure is more than 4 times larger than that of the two earlier calculations. As table 2 also shows, the mld value obtained with the Herndl and Brown model [26] is quite larger than the SLGT result, despite the fact that the two calculations use the same isospin matrix elements. A possible explanation for this result is that Herndl and Brown [26] did not take into account the small, but not negligible, state dependence of the Coulomb interaction.

Table 3. Matrix elements of the effective Hamiltonian (in MeV), obtained from the 477 level fit.

Matrix element	J,T	F-FIT	C-FIT	GF	SLGT
E_g^π		3.017	2.971	2.921	2.993
E_p^π		3.380	3.428	3.531	3.379
E_g^ν		17.35	17.32	17.91	17.34
E_p^ν		18.35	18.21	18.39	18.19
$\langle g^2\|V\|g^2\rangle$	0,1	−2.089	−2.102	−2.070	−2.039
	1,0	−1.038	−0.987	−1.322	−1.517
	2,1	−0.919	−0.922	−0.937	−0.906
	3,0	−0.785	−0.750	−0.700	−0.747
	4,1	−0.094	−0.086	−0.160	−0.106
	5,0	−0.495	−0.493	−0.447	−0.564
	6,1	0.172	0.178	0.140	0.190
	7,0	−0.447	−0.446	−0.640	−0.648
	8,1	0.311	0.322	0.241	0.321
	9,0	−1.751	−1.759	−1.752	−1.504
$\langle g^2\|V\|p^2\rangle$	0,1	0.870	0.868	0.890	0.869
	1,0	−0.327	−0.320	−0.565	0.148
$\langle gp\|V\|gp\rangle$	4,0	−1.683	−1.807	−1.319	−1.696
	4,1	0.598	0.626	0.412	0.452
	5,0	−0.469	−0.373	−0.671	−0.423
	5,1	−0.186	−0.218	−0.188	−0.077
$\langle p^2\|V\|p^2\rangle$	0,1	−1.113	−1.118	−0.774	−0.850
	1,0	−1.625	−1.246	−1.550	−1.392

The matrix elements of the effective Hamiltonian obtained from the two 477 level fits, described above, are listed in table 3 together with those of the GF and SLGT interactions. As table 3 shows, there is a strong similarity between the 4 interactions in all matrix elements in which only the $g_{9/2}$ orbital is involved. This similarity, however, ceases to exist for matrix elements involving the $p_{1/2}$ orbital, while the discrepancies are quite large for those involving the $(p_{1/2})^2$ configuration. Another example and a possible explanation of this behaviour are discussed below.

Shell-model calculations using the F-FIT and C-FIT interactions are expected to describe satisfactorily most of the observed nuclear properties of the $38 \leq Z \leq 50$ and $47 \leq N \leq 50$ nuclei and, in many cases, make useful predictions about others not yet detected. However, if one is interested in the description of a smaller number of nuclei, then these two interactions might not be the most appropriate. This is demonstrated in table 4, which shows the results obtained with the F-FIT and C-FIT interactions

Table 4. Comparison of experimental and calculated energies for selected states of the $N = 50, 49$ nuclei.

Nucl.	J^π	$E^{\rm exp}$	$E^{\rm th}$-$E^{\rm exp}$ (keV)			
		keV	F-FIT	C-FIT	S-FIT	SLG
^{91}Nb	$3/2^-$	1312	328	337	118	123
	$11/2^-$	2413	589	629	205	281
	$15/2^-$	2660	636	695	195	273
^{94}Ru	0^+	2995	−452	−423	−234	−379
^{96}Pd	10^+	3784	347	350	189	239
	12^+	4574	411	422	182	305
^{87}Sr	$1/2^-$	389	−375	−1	−237	0
^{88}Y	0^+	765	−318	−475	−137	85
^{90}Nb	1^+	382	604	612	343	124
^{92}Tc	1^+	711	620	638	266	−102
	6^+	966	−351	−351	−302	−331
^{94}Rh	17^+	4498	403	401	108	273
^{95}Pd	$29/2^+$	3999	348	338	112	268
	$33/2^+$	4679	447	445	124	332
^{98}Cd	6^+	2228	307	295	200	236
mld (keV)			161	165	113	127

for some selected levels of the $N = 50, 49$ nuclei and also includes the mld value corresponding to 211 levels of these nuclei. It should be reminded that 211 was the number of $N = 49, 50$ levels considered in the original 519 data set and 12 of them were removed in the determination of the F-FIT and C-FIT interactions. These states are now included in table 4 together with the $1/2^-$ of ^{87}Sr, the 0^+ of ^{88}Y and the 6^+ of ^{98}Cd, discussed above. Thus, table 4 includes all states which the F-FIT and C-FIT calculations fail to reproduce satisfactorily. Also shown in the table are the results of two other calculations. The first, denoted as S-FIT (special fit), uses an effective interaction specially obtained by fitting to the 211 data of $N = 49, 50$ nuclei. The other corresponds to the isospin non-conserving SLG interaction [8].

As table 4 shows, the mld values obtained by the F-FIT and C-FIT calculations for the 211 levels of the $N = 49, 50$ nuclei are quite large. This should be attributed to the inclusion in the χ^2 of states which, as table 4 shows, the two calculations reproduce badly but also to the reduction of number D in eq. (8) to 211 from the 477 value used in table 2. Not shown in table 4 are the mld values corresponding to the SLGT and GF interactions, which are 193 and 169 keV, respectively. The last value is quite close to the value obtained in the F-FIT and C-FIT results. However, a drastic reduction to mld is obtained, as table 4 shows, when the isospin non-conserving SLG interaction is used. This is a remarkable result, in view of the fact that the SLG interaction was derived using only 108 data, and can only be improved by a special fit (S-FIT) to the 211 data of the $N = 49, 50$ nuclei. This last calculation produces a vast improvement on F-FIT and C-FIT results of table 4. It should be mentioned, however, that the S-FIT interaction compares unfavourably with F-FIT and C-FIT, when applied to studies of $N = 47, 48$ nuclei.

Table 5. Matrix elements of the effective Hamiltonian (in MeV) expressed in the particle-hole formalism.

Matrix element	J	F-FIT	C-FIT	S-FIT	SLG
ϵ_g		−6.231	−6.235	−6.268	−6.248
ϵ_p		−6.952	−6.946	−7.089	−7.124
$\epsilon_{g^{-1}}$		11.096	11.113	11.206	11.113
$\epsilon_{p^{-1}}$		11.110	11.500	11.357	11.501
$\langle g^2\|V\|g^2\rangle$	0	−1.751	−1.764	−1.652	−1.705
	2	−0.627	−0.630	−0.546	−0.615
	4	0.169	0.177	0.215	0.155
	6	0.422	0.428	0.423	0.437
	8	0.563	0.574	0.551	0.570
$\langle g^2\|V\|p^2\rangle$	0	0.856	0.854	0.922	0.853
$\langle gp\|V\|gp\rangle$	4	0.866	0.894	0.714	0.716
	5	0.088	0.054	0.168	0.194
$\langle p^2\|V\|p^2\rangle$	0	−0.804	−0.809	−0.419	−0.544
$\langle gg^{-1}\|V\|gg^{-1}\rangle$	0	5.399	5.404	5.605	5.145
	1	2.750	2.802	2.676	1.945
	2	1.085	1.062	1.163	1.068
	3	0.981	0.991	0.948	0.817
	4	0.218	0.212	0.264	0.368
	5	0.264	0.257	0.287	0.331
	6	0.078	0.079	0.106	0.161
	7	0.147	0.145	0.150	0.162
	8	0.162	0.151	0.128	0.120
	9	0.908	0.889	0.904	0.934
$\langle gg^{-1}\|V\|pp^{-1}\rangle$	0	2.642	2.638	2.301	2.660
	1	−1.283	−1.464	−1.135	−1.389
$\langle gp^{-1}\|V\|gp^{-1}\rangle$	4	0.306	0.267	0.188	0.238
	5	0.521	0.561	0.521	0.297
$\langle gp^{-1}\|V\|pg^{-1}\rangle$	4	0.334	0.331	0.066	0.165
	5	−0.080	−0.082	−0.326	−0.160
$\langle pg^{-1}\|V\|pg^{-1}\rangle$	4	0.306	0.267	0.188	0.371
	5	0.521	0.561	0.521	0.569
$\langle pp^{-1}\|V\|pp^{-1}\rangle$	0	1.881	1.310	1.608	2.278
	1	1.369	1.183	1.021	1.299
E_g^π		3.017	2.971	2.981	2.992
E_p^π		3.380	3.428	3.401	3.380
E_g^ν		17.35	17.32	17.52	17.40
E_p^ν		18.35	18.21	17.35	17.29

As discussed above, all interactions determined in this work are charge-independent and this property applies to the S-FIT interaction also. Now it is interesting to observe in table 4 that there are 2 states, the 1^+ of ^{90}Nb and the 1^+ of ^{92}Tc, for which the SLG results are in much closer agreement with experiment than the S-FIT results. It has been pointed by Gross and Frenkel [9], that the ability of

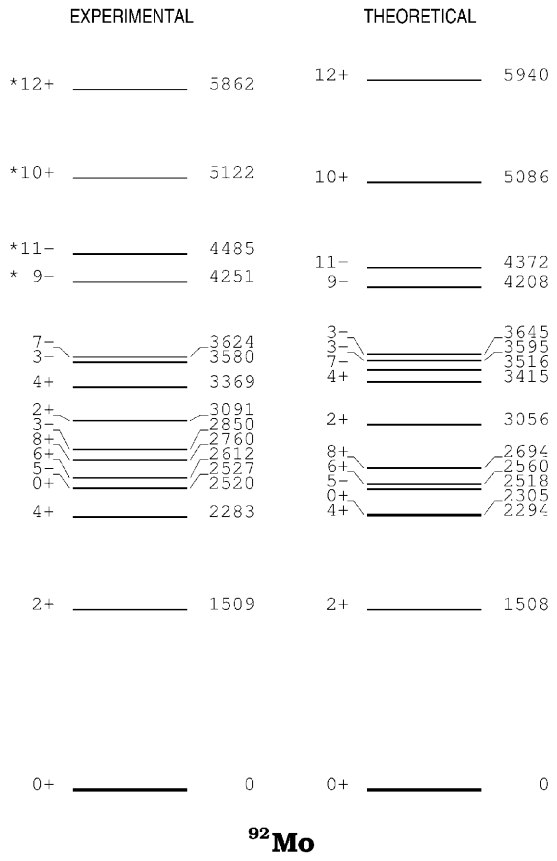

Fig. 1. Experimental and calculated levels of ^{92}Mo. Energies are given in keV.

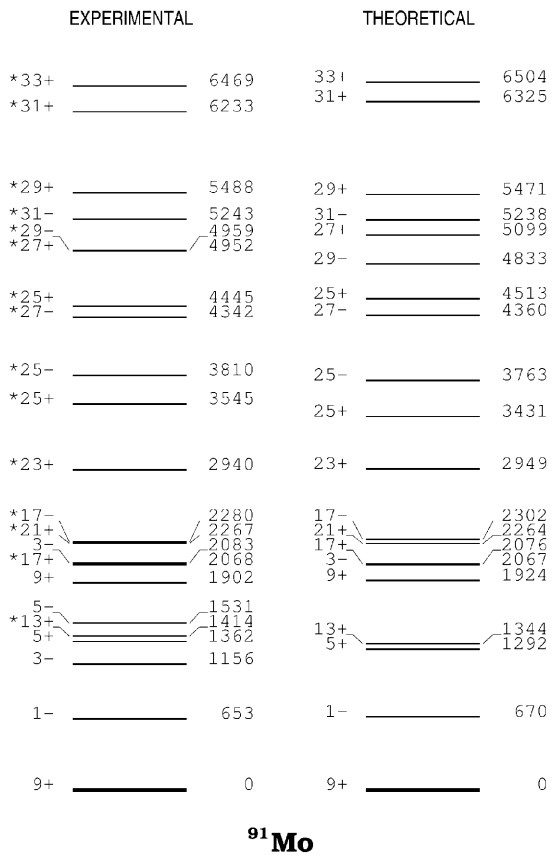

Fig. 2. Experimental and calculated levels of ^{91}Mo. Energies are given in keV.

the SLG interaction to reproduce these two 1^+ states is due to the isospin impurities in its matrix elements.

The four interactions discussed in table 4 are compared in table 5. In view of the fact that the SLG interaction does not conserve isospin, we use in table 5 the proton-neutron formalism. The particle-hole formalism is also used, so that the matrix elements listed in the table are suitable for shell-model calculations employing ^{88}Sr as core. It should also be mentioned, that the 2-particle matrix elements of table 5 represent 2-proton interaction, *i.e.* the Coulomb contibution of table 1 has been added to our 2-particle elements. At the bottom of the table we list, for comparison reasons, the single-hole energies corresponding to the ^{100}Sn core.

The remarks made with respect to behaviour of the matrix elements in table 3 apply also to those of table 5. Thus there is strong similarity among the matrix elements of the four interactions when only the $g_{9/2}$ orbital is involved, while there are discrepancies among matrix elements containing the $p_{1/2}$ orbital. The most clear example of these discrepancies appears in the last entry of table 5, where the $p_{1/2}$ neutron hole energy obtained in the S-FIT and SLG calculations appears to be about 1 MeV lower from that of the other two interactions. Such behaviour suggests that the neutron $p_{1/2}$ admixtures, in the majority of levels considered in the calculation, are too weak to be accurately determined in the fitting.

3 Results

In this section we compare with experiment some of the results obtained from our calculation. We also present some predictions of our model regarding proton-rich nuclei in the vicinity of ^{100}Sn. All the results presented in this section were obtained with the F-FIT interaction which, as described in sect. 2, produces best overall agreement with the available experimental data.

Figures 1-6 contain experimental and calculated spectra of nuclei included in the fitting procedure. These were chosen to represent all 4 classes of nuclei considered in the calculation. Thus fig. 1 shows the spectrum of the $N = 50$ nucleus ^{92}Mo, while fig. 2 that of the $N = 49$ nucleus ^{91}Mo. The spectra of the $N = 48$ nuclei ^{91}Tc and ^{92}Ru are shown in figs. 3 and 4, respectively. Finally, the spectra of the $N = 47$ nuclei ^{92}Rh and ^{90}Tc are compared with experiment in figs. 5-6. In spectra of odd nuclei, the number shown in the left of each level stands for $2J^\pi$. Also a star on the left of an experimental level denotes that the J^π assignment to this level is tentative.

As may be seen in fig. 1, the calculation reproduces, in a very satisfactory manner most observed levels of ^{92}Mo, including those with a tentative J^π assignement, up to about 6 MeV of excitation. The only exception to this agreement occurs with the 3^- state at 2.85 MeV, which the calculation predicts to be about 700 keV higher in

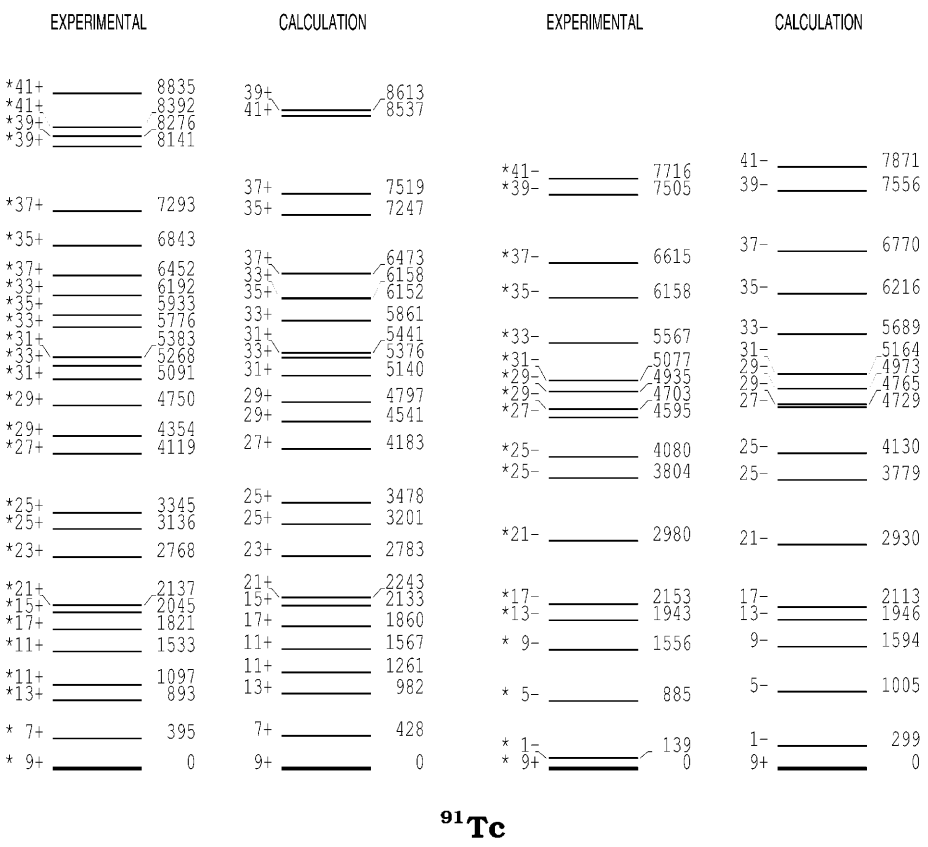

^{91}Tc

Fig. 3. Experimental and calculated levels of ^{91}Tc. Energies are given in keV.

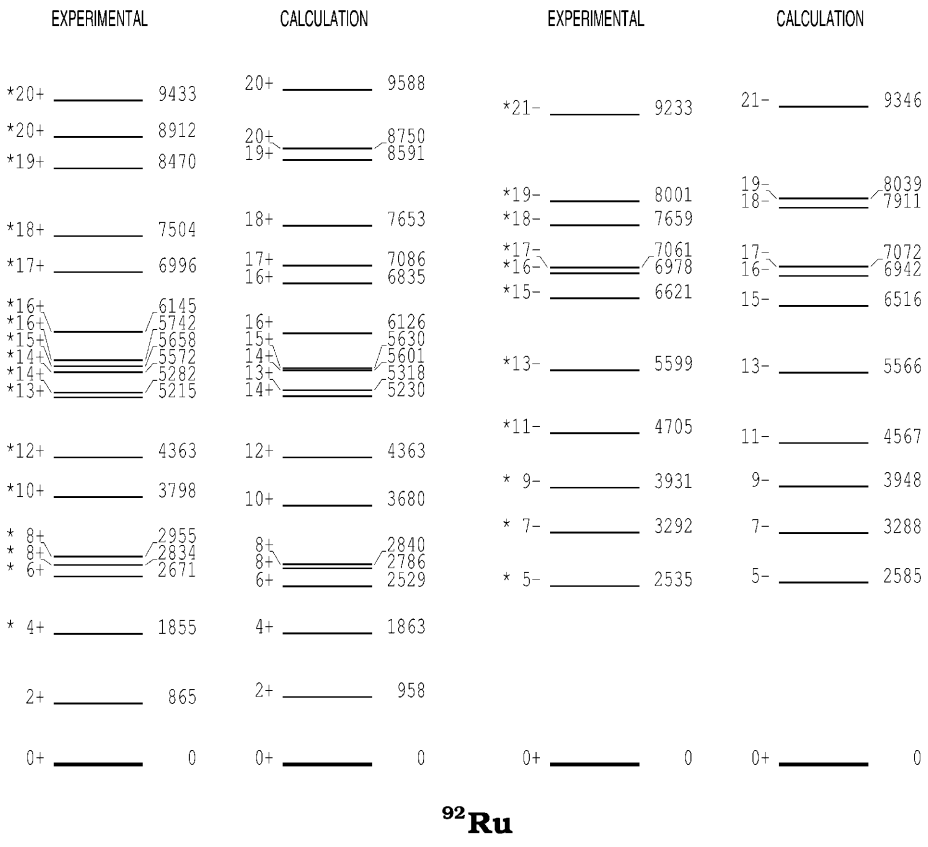

^{92}Ru

Fig. 4. Experimental and calculated levels of ^{92}Ru. Energies are given in keV.

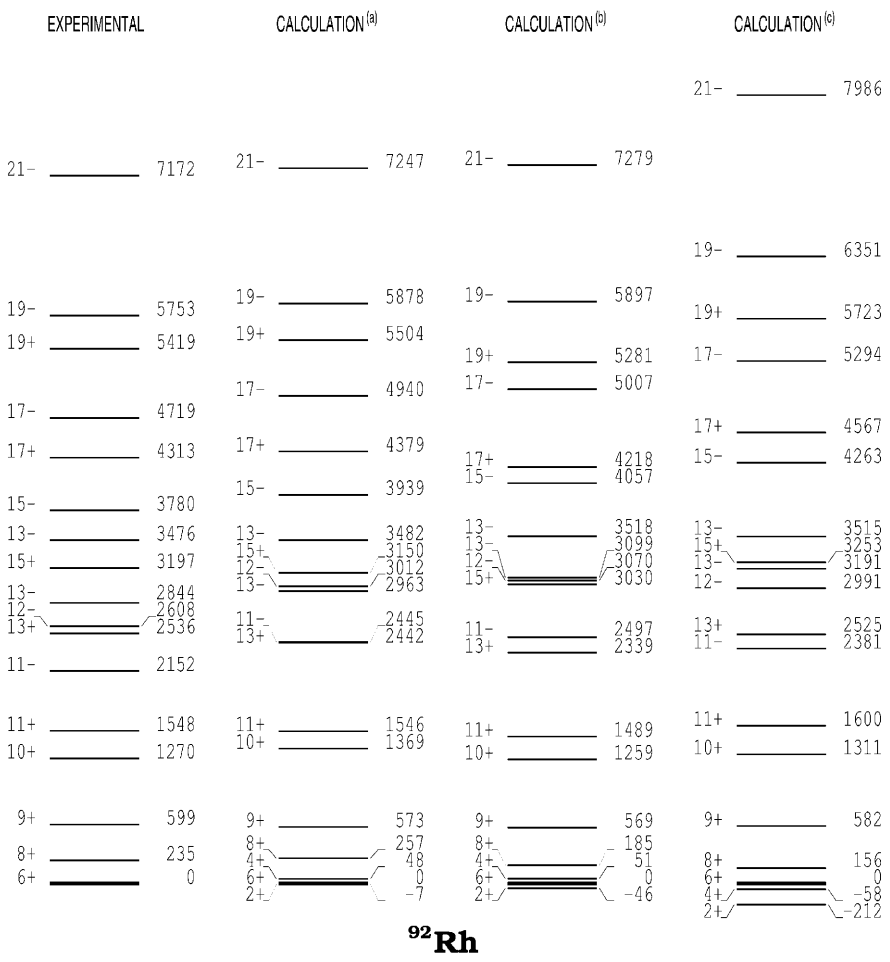

Fig. 5. Experimental and calculated levels of ^{92}Rh. The theoretical spectra marked (a) and (b) were determined using the F-FIT and GF interactions, respectively. The (c) spectrum was obtained in the calculation of Herndl and Brown [26].

excitation. This particular state is also badly reproduced in previous shell-model studies of ^{92}Mo [8,9,38] and for this reason was excluded even from the original 519 data set.

In the case of ^{91}Mo, shown in fig. 2, the calculation fails to reproduce the $3/2^-$ atate at 1.156 MeV and the $5/2^-$ at 1.531 MeV. As has been demonstrated by Sinatkas *et al.* [38], to account for these two states one needs to include in the model space the $p_{3/2}$ and $f_{5/2}$ orbitals. As fig. 2 shows, all other known states of ^{92}Mo, up to about 6.5 MeV excitation, are very accurately reproduced by the calculation.

As may be seen in fig. 3, there is a very satisfactory agreement between the experimental and theoretical spectra of ^{91}Tc. This agreement is most impressive in the case of negative parity states where, up to about 8 MeV, the difference between experimental and calculated excitation energies is, in most cases, only a few keV. In the case of positive parity states the same satisfactory agreement exists up to 6.5 MeV, while for higher excitations the differences between experimental and theoretical energies tend to increase. It appears that at such high excitation energies the effects of configurations outside the *gp*-space become evident. This is supported by the presence in the experimental spectrum, just above 8 MeV, of two possible $39/2^+$ and two possible $41/2^+$ neighbouring states. In the *gp*-space only one $39/2^+$ and one $41/2^+$ can be accounted for.

A final remark should be made about ^{91}Tc. All observed levels of this nucleus, including its ground state, have still tentative spin-parity assignments [32]. As fig. 3 shows, the results of the calculation confirm these assignments.

In the case of ^{92}Ru, shown in fig. 4, the calculation cannot describe satisfactorily the two possible 16^+ states observed to be [45] at 5.742 and 6.145 MeV. In this case the calculation is in better agreement with the results of an earlier experiment [33], where only the 16^+ state at 6.145 MeV was observed. For all other states of ^{92}Ru there is an impressive agreement between experiment and theory, as demonstrated in fig. 4. Actually, in this case a comparison between the experimental and theoretical spectra, up to about 9.5 MeV of excitation, does not provide any evidence of configurations outside the *gp*-space. Such evidence is provided only at about 11 MeV of excitation by the observation [33] of states with possible spins of 21^+,

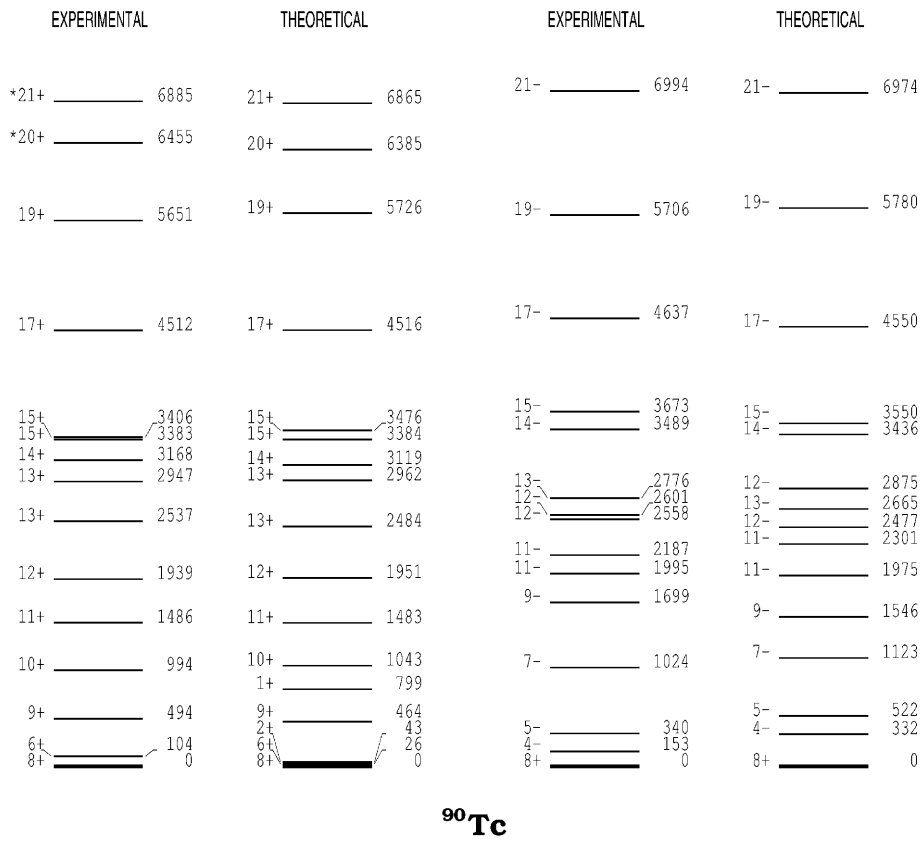

Fig. 6. Experimental and calculated levels of ^{90}Tc. Energies are given in keV.

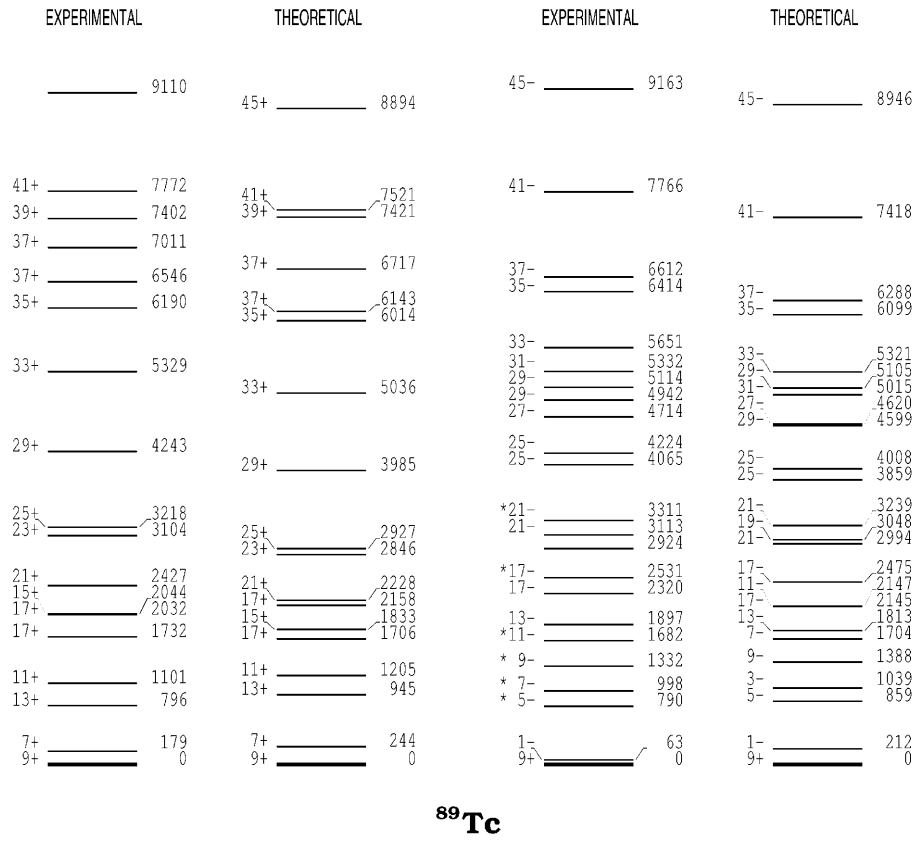

Fig. 7. Experimental and calculated levels of ^{89}Tc. Energies are given in keV.

22^- etc., *i.e.* states which cannot be described in the *gp*-space.

The $N = 47$ nucleus ^{92}Rh has recently been the subject of both experimental [23,32] and theoretical [23,26] studies. In fig. 5 we compare with the experiment the results of shell-model calculations using the F-FIT and GF interactions. Also included in fig. 5, for comparison reasons, are the results obtained by Herndl and Brown [26]. The model employed in this last calculation has been described in sect. 1.

As fig. 5 shows, up to about 5 MeV of excitation, the results of all three calculations are quite similar and in close agreement with experiment. This situation changes, however, at higher excitations. Thus the Herndl and Brown calculation [26] produces the 19^- and 21^- states at too high excitation, while the results obtained with the other two interactions remain in close agreement with experiment. This behaviour in the Herndl and Brown results should be attributed to their use of the SLGT interaction, since calculations on high-spin states of other nuclei, using this interaction, follow a similar trend to ^{92}Rh.

Another interesting feature in fig. 5 is that all calculations predict 2^+ and 4^+ low-lying states, which have not yet been observed in experiment. The case of the 2^+ state presents special interest because, if that state exists, its proximity to the ground state together with their angular momentum difference must make it a long-lived state.

The nucleus ^{90}Tc presents a special interest because of the conflicting information about its ground-state spin. Thus, the NNDC [32] compilation suggests that the ground state of ^{90}Tc is a 1^+ state while Rudolph *et al.* [13] observed a 8^+ lowest state. The results of our calculation, as well as of calculations using the SLGT and GF interactions, support the 8^+ assignment to the ground state. Thus the lowest 1^+ state of ^{90}Tc is predicted to be 457 keV (SLGT), 915 keV (GF) or 799 keV (our result) above the 8^+ state. For this reason the spectrum of ^{90}Tc, shown in fig. 6, has been drawn on the assumption that the ground state is a 8^+ state.

As seen in fig. 6, the agreement between the theoretical and experimental spectra of ^{90}Tc is most satisfactory. Thus all states observed in experiment are accounted for by the calculation, while the difference between experimental and calculated energies is, in most cases, less than 100 keV. It should be noted that the calculation predicts several other states which have not yet been observed in experiment. The most notable of these states is the lowest 2^+ predicted to be only 43 keV above the ground state. If the presence of such a state, at about the predicted energy, is confirmed in future experiments then this 2^+ must constitute the case of an isomeric state.

In all figures presented so far, most of the energy levels shown were included in the fitting procedure. Thus, the observed agreement between theory and expreriment gives a more detailed description of the quality of the fit from that already presented in table 2. However, a very useful test of our interaction would be to use it to calculate spectra of nuclei not included in the fitting. The results of such a calculation are presented in fig. 7, which shows the experimental [21] and theoretical spectra of the $N = 46$ nucleus ^{89}Tc. As this figure shows, the calculation fails to reproduce satisfactorily the two observed levels at 998 and 1682 keV, for which there is a tentative J^π assignement of $7/2^-$ and $11/2^-$, respectively. However, calculations using the GF and SLGT [26] interactions also show a similar failure. For all other states of ^{89}Tc the agreement between experiment and theory is very satisfactory, although not as impressive as that of the previous figures.

Of course, the agreement between experiment and theory could be improved if the levels of ^{89}Tc, together with those of other $N = 46$ nuclei, were included in the fitting. However, as pointed by Rudolph *et al.* [13] and recently by Kalindo *et al.* [27], the low-lying states of $N = 46$ nuclei show a collective character which is difficult to describe by a shell-model calculation in a very small space.

As discussed in sect. 2, the binding energies of the $38 \leq Z \leq 50$, $47 \leq N \leq 50$ nuclei were considered in the determination of the effective interaction. Table 6 shows a comparison between experimental [44] and calculated binding energies. In this table the symbol # denotes that the experimental value was deduced from systematic trends. Such values were not included in the fitting procedure.

To determine binding energies in a shell-model calculation, one needs to know the experimental ground-state energy of the core state. In our case this was not possible since, as table 6 shows, there is still great uncertainty about the experimental binding energy of ^{100}Sn. For this reason, binding energies were calculated with respect to ^{88}Sr in the following manner:

$$BE_A^{\rm cal} = -(E_A^{\rm cal} - E_{^{88}{\rm Sr}}^{\rm cal}) + 768.467 \ {\rm MeV}, \qquad (9)$$

where A is the nucleus under study, $E_A^{\rm cal}$ its calculated ground-state energy, while 768.467 MeV is the experimental [44] binding energy of ^{88}Sr which, as table 6 shows, is known with great accuracy.

As table 6 shows, there is a satisfactory agreement between experimental and calculated binding energies, in all cases where the experimental value is measured. Thus, out of 27 such cases, only in 4 the difference between experimental and calculated values exceeds 200 keV. It is interesting to observe that near the end of the table, where proton-rich nuclei are listed, the calculation produces, generally, larger values than those deduced from systematic trends. A similar feature was also observed in a recent shell-model study by Johnstone and Skouras [41]. The possibility that systematic trends might underestimate the binding energies of proton-rich nuclei is supported by the recent measurement of the mass of ^{100}Sn [46], which gives the value of (825.785 ± 0.900) MeV for the binding energy of that nucleus.

We conclude this section by describing the predictions of the calculation on isomeric states. We have already discussed two possible such states, *i.e.* the low-lying 2^+ states of ^{92}Rh and ^{90}Tc. Another possibility is a 4^+ state of ^{88}Nb which the calculation predicts to be only 66 keV above the ground state 8^+. Another very interesting case occurs in ^{93}Pd, where the calculation predicts the ground state to

Table 6. Experimental and calculated binding energies (in MeV) of $47 \leq N \leq 50$ nuclei. All experimental data are taken from the 1995 mass tables [44]. The symbol # denotes an estimate from systematic trends.

Z	Nucleus	$BE^{\rm exp}$	σ		$BE^{\rm cal}$
38	^{85}Sr	737.436	0.003		737.228
	^{86}Sr	748.926	0.002		748.860
	^{87}Sr	757.354	0.002		757.368
	^{88}Sr	768.467	0.002		768.467
39	^{86}Y	742.904	0.014		743.004
	^{87}Y	754.910	0.003		754.850
	^{88}Y	764.062	0.003		764.143
	^{89}Y	775.538	0.003		775.419
40	^{87}Zr	750.250	0.008		750.106
	^{88}Zr	762.606	0.010		762.544
	^{89}Zr	771.923	0.005		771.958
	^{90}Zr	783.893	0.002		783.820
41	^{88}Nb	754.620	0.200	#	754.448
	^{89}Nb	766.851	0.040		767.028
	^{90}Nb	777.000	0.005		777.033
	^{91}Nb	789.052	0.003		789.041
42	^{89}Mo	760.492	0.015		760.509
	^{90}Mo	773.728	0.006		773.724
	^{91}Mo	783.836	0.011		783.866
	^{92}Mo	796.508	0.004		796.397
43	^{90}Tc	763.988	0.240		763.713
	^{91}Tc	776.829	0.200		777.076
	^{92}Tc	787.855	0.026		787.893
	^{93}Tc	800.595	0.004		800.552
44	^{91}Ru	768.647	0.500		768.506
	^{92}Ru	782.548	0.300	#	782.596
	^{93}Ru	793.479	0.090		793.509
	^{94}Ru	806.849	0.013		806.785
45	^{92}Rh	770.716	0.400	#	770.726
	^{93}Rh	784.597	0.400	#	784.764
	^{94}Rh	796.438	0.450	#	796.486
	^{95}Rh	809.910	0.150		809.874
46	^{93}Pd	774.345	0.400	#	774.060
	^{94}Pd	789.066	0.400	#	789.107
	^{95}Pd	800.937	0.400	#	800.885
	^{96}Pd	815.039	0.150		815.024
47	^{94}Ag	775.234	0.500	#	775.569
	^{95}Ag	790.105	0.400	#	790.053
	^{96}Ag	802.406	0.400	#	802.884
	^{97}Ag	816.938	0.400	#	817.036
48	^{96}Cd	793.394	0.500	#	793.144
	^{97}Cd	805.965	0.500	#	805.949
	^{98}Cd	820.897	0.210	#	821.117
49	^{99}In	821.636	0.500	#	821.969
50	^{100}Sn	824.875	0.430	#	825.040

be a $7/2^+$ state but only 3 keV above it is a $9/2^+$ state. Whichever of these two states is the excited state it must be a very long-lived one. Finally isomeric states are predicted to exist in the odd-odd proton-rich nuclei ^{96}Ag, ^{94}Ag and ^{98}In. In ^{96}Ag the ground state is predicted to be a 2^+ state but only 90 keV above is a 8^+. Again the real order of the 2 states is immaterial, since the excited one must be isomeric. In both ^{94}Ag and ^{98}In the calculation predicts the ground state to be a 0^+. The first excited state in ^{94}Ag is predicted to be a 7^+ at 760 keV, while in ^{98}In a 9^+ at 626 keV.

4 Discussion

In this paper we presented results on effective interactions which are appropriate for shell-model studies in the *gp*-space. These interactions were determined by a least-square fit to 477 observed levels of $38 \leq Z \leq 48$ and $47 \leq N \leq 50$ nuclei.

The least-square fit method appears to be the most suitable for determining the effective interaction for the *gp*-space because of the proximity in energy of the $g_{9/2}$ and $p_{1/2}$ orbitals to the other orbitals of the fp and gds shells. Thus, due to this proximity, an attempt to derive the effective interaction for the *gp*-space by perturbation techniques [38] produced very unsatisfactory results.

The results of our calculation, presented in sect. 3, are, in most cases, in very satisfactory agreement with experiment. Thus, the interactions determined in this work may be considered as improved versions of the earlier SLG and GF interactions. This is due to the fact that our calculation used a much larger set of experimental data than that considered in the two earlier ones.

There are problems in any attempt, like ours, to fit simultaneously the observed spectra of nuclei in the wide $85 \leq A \leq 100$ mass range. One of the problems occurs because of the different behaviour of nuclei at the two ends of the *gp*-space. Thus it is known, both experimentally [32] and theoretically [38], that the wave functions of nuclei at the lower end of the *gp*-space contain appreciable admixtures from the $p_{3/2}$ and $f_{5/2}$ orbitals. On the other hand, Johnstone and Skouras [40] have recently demonstrated the role of particle-hole excitations, from the *gp*-space to the $(g_{7/2}, d_{5/2}, d_{3/2}, s_{1/2})$ space above, in nuclei near mass $A = 100$. It is not certain that a fitting calculation, which only treats the projections of the true wave functions onto the model space, can simultaneously take care of both these two types of admixtures.

Another, but related, problem has to do with the inclusion in the fitting of nuclei with quite different number of neutrons, *i.e.* $N = 50$ to $N = 47$. Now, because of the Pauli blocking effect, particle-hole excitations, from either the fp or to the gds shells, are expected to have different importance on nuclei with different valence neutrons.

It is, possibly, because of these two problems that the calculation fails to describe satisfactorily(F-FIT case) the spectra of two nuclei which in the *gp*-space have a very simple description. These are ^{87}Sr, i,e a single neutron-hole nucleus with respect to ^{88}Sr, and ^{98}Cd, which is

described in terms of two proton holes with respect to ^{100}Sn. As described in sect. 2, the ^{87}Sr case can be improved by means of constraints (C-FIT), but this produces a deterioration on the agreement with experiment for the 0^+ state of ^{88}Y. However, this conflict between ^{87}Sr and ^{88}Y results is most probably due to the inclusion of $N = 47$–48 data, since a fitting of only the $N = 50$–49 energy levels (S-FIT) reproduces satisfactorily both the $1/2^-$ of ^{87}Sr and the 0^+ state of ^{88}Y.

It is important to note that our calculation, with the exception of SLGT, uses a smaller number of parameters, *i.e.* only 22, compared to previous determinations of the effective interaction in the *gp*-space [8,9]. Moreover, the nuclear part of our 2-body interaction strictly conserves isospin. This property was not observed in the SLG calculation [8], or was only approximately introduced in the GF interaction, by means of constraints of weight 3 [9].

Although the idea of producing a charge-independent interaction is very attractive, perhaps it should be abandoned in future determinations of the effective Hamiltonian in the *gp*-space. Thus if, following the SLG approach [8], the proton, neutron and proton-neutron matrix elements are treated as independent, then the number of parameters would increase to 42. This number is still less than 10% of the currently available experimental data. However, the increase of the number of independent parameters to 42 from 22 would, most probably, produce a better agreement between experiment and theory than that obtained in this work. Another interesting aspect of such a project would be to examine the degree of charge-independence violation in the *gp*-space.

The authors wish to thank Dr. C.A. Kalfas for his valuable assistance in the preparation of this manuscript.

References

1. I. Talmi, I. Unna, Nucl. Phys. **19**, 225 (1960).
2. S. Cohen, R.D. Lawson, M.H. MacFarlane, M. Soga, Phys. Lett. **10**, 195 (1964).
3. N. Auerbach, I. Talmi, Nucl. Phys. **64**, 458 (1965).
4. J. Vervier, Nucl. Phys. **75**, 17 (1966).
5. J.B. Ball, J.B. McGrory, R.L. Auble, K.H. Bhatt, Phys. Lett. B **29**, 182 (1969).
6. J.B. Ball, J.B McGrory, J.S. Larsen, Phys. Lett. B **41**, 581 (1972).
7. D.H. Gloekner, F.J.D. Serduke, Nucl. Phys. A **220**, 477 (1974).
8. F.J.D. Serduke, R.D. Lawson, D.H. Gloekner, Nucl. Phys. A **256**, 45 (1976).
9. R. Gross, A. Frenkel, Nucl. Phys. A **267**, 85 (1976).
10. A. Amusa, R.D. Lawson, Z. Phys. A **307**, 33 (1982); **314**, 314 (1983).
11. J. Blomquist, L. Rydstrom, Phys. Scr. **31**, 31 (1985).
12. S.E. Arnell *et al.*, Phys. Scr. **47**, 142 (1993).
13. D. Rudolph *et al.*, Phys. Rev. C **47**, 2574 (1993).
14. A. Bödeker *et al.*, Phys. Rev. C **48**, 1617 (1993).
15. M. K. Kabadiyski *et al.* Phys. Rev. C **50**, 110 (1994).
16. D. Rudolph *et al.*, Phys. Rev. C **49**, 66 (1994).
17. M. Weiszflog *et al.*, J. Phys. G **20**, L77 (1994).
18. J. Heese *et al.*, Phys. Rev. C **49**, 1896 (1994).
19. M. Gorska *et al.*, Z. Phys. A **353**, 233 (1995).
20. D. Zainea *et al.*, Z. Phys. A **352**, 365 (1995).
21. D. Rudolph *et al.*, Nucl. Phys. A **587**, 181 (1995).
22. R. Schubart *et al.*, Nucl. Phys. A **591**, 515 (1995).
23. D. Kast *et al.*, Z. Phys. A **356**, 363 (1997).
24. D. Rudolph *et al.*, Phys. Scr. T **56**, 120 (1995).
25. D. Rudolph, K.P. Lieb, H. Grawe, Nucl. Phys, A **597**, 298 (1996).
26. H. Herndl, B.A. Brown, Nucl. Phys. A **627**, 35 (1997).
27. E. Kalindo, A. Jungclaus, K.P. Lieb, Eur. Phys. J. A **9**, 439 (2000).
28. K. Ogawa, Phys. Rev. C **28**, 958 (1983).
29. K. Schmidt *et al.*, Z. Phys. A **350**, 99 (1994).
30. K. Schmidt *et al.*, Nucl. Phys. A **624**, 185 (1997).
31. K. Schmidt *et al.*, Eur. Phys. J. A **8**, 303 (2000).
32. National Nuclear Data Center, Brookhaven National Laboratory, N.Y, USA, 2001.
33. S.E. Arnell *et al.*, Z. Phys. A **346**, 111 (1993).
34. S.E. Arnell *et al.*, Phys. Rev. C **49**, 51 (1994).
35. H.A. Roth *et al.*, Phys. Rev. C **50**, 1330 (1994).
36. K. Fujita, T. Komoda, Prog. Theor. Phys. **60**, 178 (1977).
37. X. Ji, B.H. Wildenthal, Phys. Rev. **37**, 1256 (1988); **38**, 2849 (1988); **40**, 389 (1989).
38. J. Sinatkas, L.D. Skouras, D. Strottman, J.D. Vergados, J. Phys. G **18**, 1377 (1992); **18**, 1401 (1992).
39. K. Muto, T. Shimano, H. Horie, Phys. Lett. B **135**, 349 (1984).
40. I.P. Johnstone, L.D. Skouras, Phys. Rev. C **55**, 1227 (1995).
41. I.P. Johnstone, L.D. Skouras, Phys. Rev. C **51**, 2817 (1995).
42. S.P. Pandya, Phys. Rev. **103**, 956 (1956).
43. P.J. Brussaard, P.W.M. Glaudemans, *Shell-model Applications in Nuclear Spectroscopy* (North-Holland Publishing Company, Amsterdam, New York, Oxford, 1977) p. 100.
44. G. Audi, A.H. Wapstra, Nucl. Phys A **595**, 409 (1995).
45. C. Lingk *et al.*, Phys. Rev. C **56**, 2349 (1997).
46. M. Chartier *et al.*, Phys. Rev. Lett. **77**, 2400 (1996).